

Surface Structure of Amorphous Polystyrene: Comparison of SFM Imaging and Lattice Chain Simulations

G. Goldbeck-Wood

Accelrys, 230/250 The Quorum, Barnwell Road, Cambridge CB5 8RE, U.K.

V. N. Bliznyuk,[†] V. Burlakov, H. E. Assender, G. A. D. Briggs, and Y. Tsukahara

Department of Materials, University of Oxford, Oxford OX1 3PH, U.K.

K. L. Anderson* and A. H. Windle

Department of Materials Science and Metallurgy, University of Cambridge, Cambridge CB2 3QZ, U.K.

Received November 13, 2001; Revised Manuscript Received March 1, 2002

ABSTRACT: We identify and characterize surface features on the length scale 1–100 nm on a free equilibrated surface of amorphous polystyrene (in contact with air), from a combination of scanning force microscopy and coarse-grained polymer simulation techniques. By carrying out a lateral autocorrelation analysis of the experimental and simulated surface height profiles, we find characteristic length scales of structural organization of polymer chains depending on their molecular mass in the range 3.9 kg/mol to 9 Mg/mol. The lateral autocorrelation functions exhibit an initial exponential decay, which corresponds to a correlated arrangement of several monomer segments at the surface of the amorphous polymer, followed by one or more peaks. The same autocorrelation analysis of the surface height data is applied to the simulated data created for the same system with a lattice chain model. By combining evidence of simulation and experiment results, we deduce that a characteristic feature in the surface autocorrelation function has a length scale close to the radius of gyration over several decades of molecular weight. This study therefore opens up new ways of characterizing polymer surfaces and even observing the polymer radius of gyration directly.

Introduction

Although theoretical models of conformational behavior of polymer chains were originally developed for amorphous polymers (for example, scaling concept, fractals),^{1–3} the structure and properties of the surface of amorphous polymers are less well understood than those of crystalline polymers. At the same time, the strong trend toward nanoscale-structured materials means that to an increasing extent materials will be characterized by their surface and interface properties rather than by their bulk properties. The well-established structural techniques for crystalline polymer surfaces (such as grazing incidence X-ray diffraction and electron diffraction) are not so suitable for amorphous (less organized) surfaces, and so the organization of amorphous polymers at the surface presents particular challenges to both experimental studies and computer simulation methods.

Theory predicts the existence of only relatively short-range (one to two monomer segment distances) interactions for the bulk amorphous polymer material,⁴ which has been proven by direct diffraction experiments. In other words, polymer chain entanglements effectively screen longer interactions. However, this screening is different at the surface, due to the asymmetry of polymer chains near the air interface (Figure 1). One can therefore expect an appearance of two types of correlations at the polymer surface: short-range (“bulk type”) correlations, and larger scale correlations on a level corresponding to macromolecular chain length (on

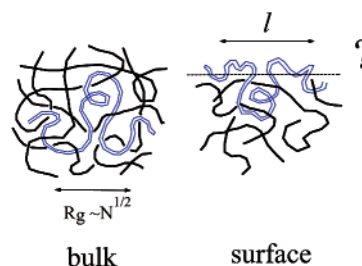


Figure 1. Comparison of structural organization and characteristic dimensions of an amorphous polymer material in the bulk and at the surface.

the order of a radius of gyration). Theoretical considerations also predict intermediate states (“blobs”) with typical dimensions on the order of several monomer segments.^{5,6} The reality of blobs is supported by experimental observations.⁷

Scanning force microscopy (SFM) techniques have become available as a powerful tool for studies of morphology and physical properties of polymer materials on the surface. This has stimulated a reconsideration of many physical phenomena that occur at the surface and is giving a new impulse for critical review of some basic principles of the structural organization of polymers.⁸ Computer simulations provide an excellent tool for probing the structural organization of materials (including polymers) on various levels of complexity. Since the size scale of structure at the polymer surface is on the order of the radius of gyration of the chains, classical atomistic simulation methods are ruled out. Coarse-grained lattice chain methods have recently been used to very good effect to probe polymer structure at this level, including effects of entanglement.^{9,10}

[†] Present address: CMD Department, Western Michigan University, Kalamazoo, MI 49008.

In this paper, we address the question of the structural organization at the surface of a typical amorphous polymer, atactic polystyrene (aPS), by means of direct structural investigation by high-resolution SFM accompanied by statistical analysis with the autocorrelation function approach. Simultaneously, aPS is simulated by means of a face centered cubic (fcc) lattice chain model. Using similar mathematical analyses and an overlapping range of molecular masses studied allows direct comparison of the theoretical and experimental results.

Experimental Section

We have used SFM to study the surface structure of amorphous atactic polystyrene (aPS) as a function of molecular mass M_n for a set of aPS samples chosen to cover more than 3 orders of magnitude in M_n (3900 to 9 000 000). The aPS samples were obtained from Polymer Source, Inc. (Dorval, Quebec, Canada). The polydispersity index (the ratio of the weight-averaged molecular weight, M_w , to the number-averaged molecular weight, M_n) was below 1.15 for all the polymer fractions under study, and typically did not exceed 1.05. Samples were deposited by spin coating from a toluene solution on a glass or silicon substrate to form films whose thickness h was much greater than the radius of gyration R_g of the molecules (1.7–50 nm for the aPS set under investigation). As was shown earlier, even ultrathin spin coated films may still contain a considerable amount of the solvent.¹¹ It is important to anneal the samples sufficiently to remove any traces of the solvent as well as for equilibration of the surface structure. Our polymer films were therefore annealed for at least 2 h at 110 °C before SFM experiments. Our previous study of amorphous polymer surface structure revealed that such a temperature and time scale was sufficient for achieving structural equilibrium.¹²

The samples were examined using an Autoprobe CP (Park Scientific) atomic force microscope operated in tapping mode to scan over surface areas between $300 \times 300 \text{ nm}^2$ and $5 \times 5 \text{ }\mu\text{m}^2$. An autocorrelation function analysis, described below, was applied to quantitatively characterize the polymer surface topography. Typically, surface areas of $1 \times 1 \text{ }\mu\text{m}^2$ were chosen as the most suitable for the ACF analysis, which was implemented in a MAPLE-based program.¹² The autocorrelation function (ACF) can be used for the statistical description of amorphous systems.^{3,13} In many cases the autocorrelation function can be approximated by an exponential decay, and it can then be characterized by a single autocorrelation length ξ at which $\text{ACF} = 1/e$:

$$\text{ACF} \sim \exp(-x/\xi) \quad (1)$$

This structural parameter indicates an average distance from an arbitrary point in the sample beyond which the correlation in arrangement of the structural units is lost.

Simulation

Description of the Model. A simulation method is needed which links to the necessary level of detail of the underlying system yet can handle polymer structures both below and considerably above the entanglement molecular weight. In recent work, it has been demonstrated that the fcc lattice chain model can indeed meet these requirements.⁹ In the model, each polymer chain is composed of connected sites, each site containing a short section of the polymer chain, on a three-dimensional face centered cubic (fcc) lattice. Vacant sites occupy a percentage of the lattice, with motion of chain segments facilitated by exchange of these vacant sites with sites that represent the polymer chain. Pairs of

neighboring sites are selected at random and a move is allowed if one of the sites is a vacancy and the chain is not permanently broken by the exchange. The exchange of sites will be accepted if the chain is broken initially in one place, provided the chain can relax to reconnect the chain within the attempted move step. Further details can be obtained from a previous publication.⁹ At each Monte Carlo step a lattice site is selected as the first site of an attempted move. During one MC step, multiple vacancy–segment exchanges occur, potentially resulting in overall change in the configuration of each polymer chain with no lattice site being doubly occupied.

Parameterization of the Model. As we aim to simulate a specific polymer in a specific environment, i.e., a film of atactic polystyrene, the model is parameterized to reflect this situation. The parameterization takes three steps. Model parameters must be chosen to achieve (i) the correct density, (ii) the correct end-to-end distance, and (iii) polymer–air coexistence. For the first two steps, we followed a routine described in an earlier publication.⁹

(i) Density: In our model, chains made up of segments representing a certain number of monomers each reside on an fcc lattice. Taking the chain parameters and lattice geometry into account, a relationship between the occupancy O and the density can be derived:

$$O = \frac{\rho N_A a_{\text{seg}}^3}{\sqrt{2} M_{\text{mon}}} n_{\text{mon}}^2 \quad (2)$$

Here ρ is the polymer density, N_A is Avogadro's number, a_{seg} is the length of a segment, n_{mon} is the number of monomers in a segment, and M_{mon} is the molecular weight of a single monomer. It can be seen immediately that there can be several possible choices for the number of monomers in a segment. The criteria for occupancy of the lattice chain model, representing a bulk polymer, are that the occupancy should be high, but must of course be less than one. In the present case, this can be satisfied by choosing $n_{\text{mon}} = 4$. The average segment length for a 4mer was determined as 0.9 nm, by means of the RMMC (rotational isomeric state Metropolis Monte Carlo) and Synthia modules on the Cerius² software from Accelrys. The other quantities in eq 2 are $\rho = 1.074 \text{ g cm}^{-3}$ and $M_{\text{mon}} = 104.15 \text{ g mol}^{-1}$. As a result, eq 2 yields an occupancy $O = 0.8$. Therefore, an fcc lattice model of occupancy 0.8 can be regarded as a coarse-grained representation of polystyrene, with each chain segment representing four styrene monomers. We note that (a) the density matching has introduced a length scale into the model and (b) this type of coarse graining amounts to about a factor of 10 in size scale.

(ii) A further important chain characteristic to be maintained at the coarse grained level is the end-to-end distance. To adjust the model to the experimentally known end-to-end distance, an energy term is introduced as a function of angle ϕ between successive chain segments, i.e., a "lattice bond angle energy" (Figure 2):

$$E(\phi) = E_a \cos \phi \quad (3)$$

Since only a discrete set of angles (60, 90, 120, 180°) is allowed due to the fcc lattice, the energy also takes discrete values. These energies are taken into account in the Metropolis Monte Carlo scheme used to move chain segments. Increasing E_a leads to an increase in

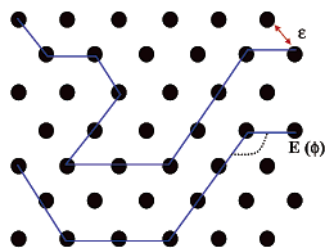


Figure 2. Two-dimensional sketch of the fcc lattice model, indicating lattice chains, the angle energy, and the “cohesive energy” ϵ .

Table 1

experiment (SPM)		simulation	
M_n	polydispersity index M_w/M_n	no. of segments $\sim M_n/(4M_{\text{mon}})$	polydispersity index
3900	1.11	10	1
9300	1.13	20	1
20 800	1.07	41	1
34 000	1.06	82	1
		164	1
115 900	1.04	240	1
347 000	1.06		
965 000	1.15		
1 340 000	1.05		
6 000 000	1.22		
9 000 000	1.22		

the average end-to-end distance R . The target value of R in the model was determined from

$$R_L^2 = C_\infty N \alpha_{\text{mon}}^2 \quad (4)$$

where $C_\infty \approx 9.8$ ¹⁶ is the characteristic ratio of atactic polystyrene, and $\alpha_{\text{mon}} = 0.25$ nm is the monomer bond length. This was achieved by choosing $E_a = 520 k_B T$.

(iii) Finally, polymer–air (represented here by vacancies for simplicity) and polymer–substrate interactions must be specified. “Cohesive energy” terms, in the form of polymer–vacancy interaction parameters, were introduced such that the bulk of the polymer retained the correct density (or occupancy) in a simulation box with a polymer surface (Figure 2). This was achieved by a pairwise interaction energy between nearest neighbor polymer and vacancy sites of $\epsilon = +36 k_B T$. Likewise, an attractive interaction energy of $\epsilon = -36 k_B T$ between polymer and substrate was introduced to ensure the polymer/substrate interface remains intact.

The simulation lattice was $32 \times 128 \times 48$ in the I, J, K dimensions. Periodic boundary conditions were used in the I, J dimensions. The K dimension was large enough so that the energies from the substrate and free top surface did not influence motion within the bulk sample. Interactions between the bottom surface and the polymer chains were independent of interactions on the free surface of the simulation.

The simulations were annealed over times considerably longer than their relaxation times (on the order of N^3 MC steps), to generate starting ensembles as random as possible, and independent simulations for each chain length were run for statistical averaging. Simulated chain lengths (N) representing specific polystyrene MW's are summarized in Table 1. Empty cells represent situations where a direct comparison between the simulation and experiment was either not feasible computationally or where it was not possible to acquire experimental samples.

Length Scales. For polymer systems with a hierarchy of structural organization, more than one characteristic length scale is expected: a length scale associated with the quasi-periodical arrangement of structural subunits and a characteristic distance of the mutual coupling in such an arrangement. In polymer systems (long chain molecules) such distances of mutual influence in the arrangement of structural elements might correspond to the characteristic dimensions of macromolecules: the size of molecular coils and subcoils (blobs).⁴ Capillary waves might add complexity to this picture if we were to measure areas on the order of several mm squared on the surface.¹⁴

Independently, the radius of gyration (R_g) can be calculated using geometrical dimensions of polymer chains, and used as a parameter to characterize natural dimensions of macromolecular coils in the bulk. The orientation distribution (Q) is used to determine the surface contribution to chain conformations, and is given by

$$Q_{Z_k} = \frac{3 \cdot \langle R_z^2 \rangle_k - \langle R^2 \rangle_k}{2 \langle R^2 \rangle_k} \quad (5)$$

where R_z is the K -component of the chain's end-to-end vector, which has a center of mass at the particular K position in the fcc lattice. R is the chain's average end-to-end vector for all chains whose center of mass is also at the K position within the simulation box, described by

$$R^2 = R_x^2 + R_y^2 + R_z^2 \quad (6)$$

Assuming the chain is random in character, the end-to-end distance relates to the R_g as

$$\langle R_g \rangle = \frac{\langle R \rangle}{\sqrt{6}} \quad (7)$$

Considering this simple relation, to talk about the components of the R_g or Q is essentially the same.

Results

Figure 3 shows representative topography images obtained in tapping mode for some of the PS film surfaces, with a decade spread in the mean dimensions of the polymer chains. The vertical scale of images is different and increases with the molecular weight. This observation gives us a hint of a fractal character of the polymer surface vs the polymer chain length for the polymer under study, though we will not endeavor to discuss this in detail now. Further insight into structural organization at the surface can be achieved by considering the cross section (height profiles) of the images. A typical profile is shown in Figure 4 and demonstrates a presence of at least two characteristic length-scales within the considered scan size. This kind of height distribution was observed at an appropriate scale for each of the polymer fractions in this study. By analogy to the more ordered latex particle crystal systems considered before,¹⁵ we can ascribe these two characteristic features to a different length scale of molecular organization in the system.

Figure 5 displays ACF analysis of SFM images for several polystyrene surfaces. All the curves exhibit an initial exponential decay, which can be characterized

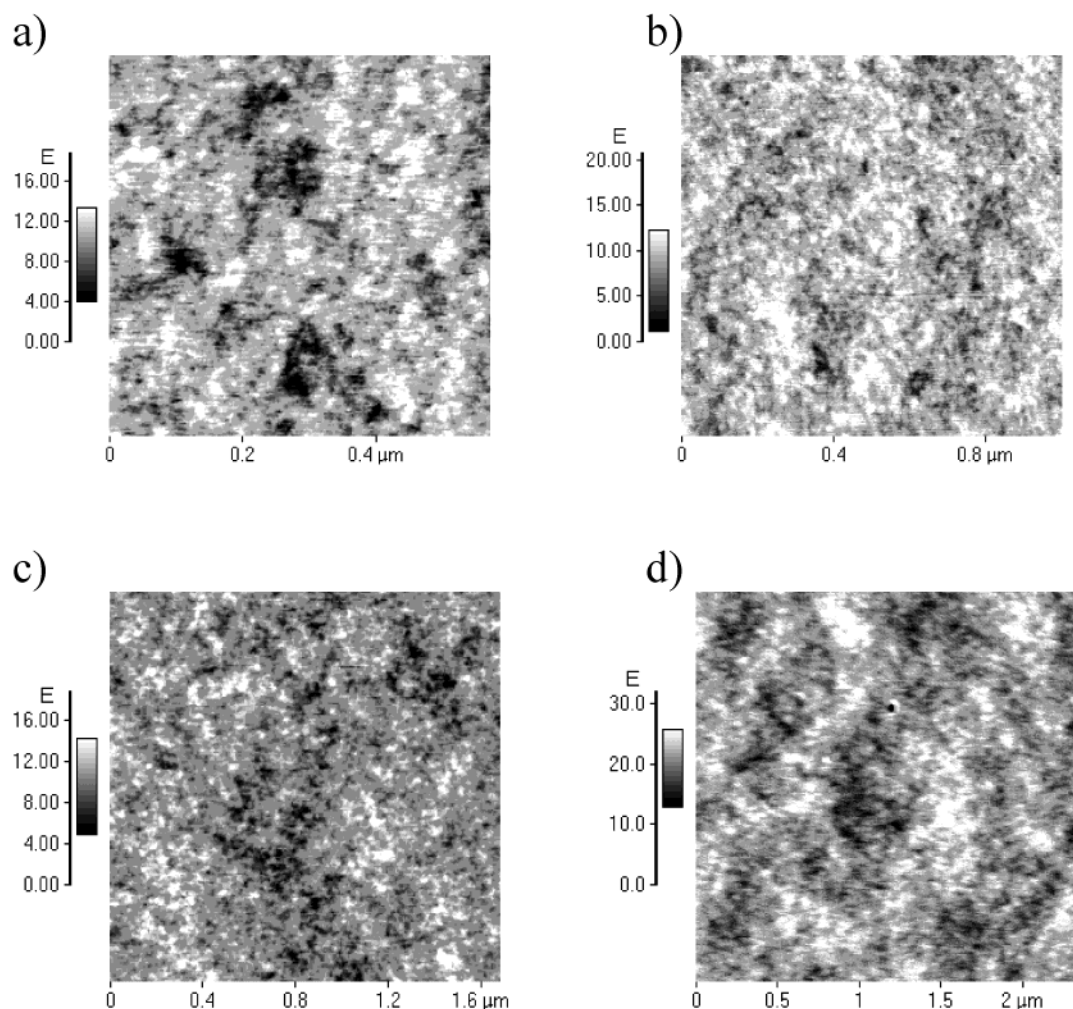


Figure 3. Tapping mode AFM images of the surface of PS samples with M_n : 10K (a), 116K (b), 1340K (c), and 6000K (d). Vertical scale is in angstroms on all images.

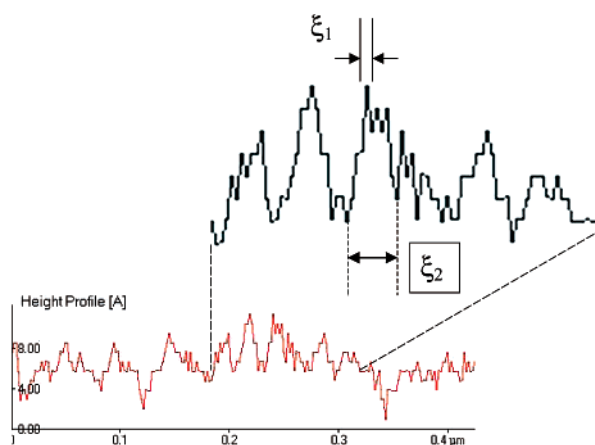


Figure 4. Height profile corresponding to image in Figure 3b. Inset shows part of the scan line at higher magnification demonstrating both fractality of the surface and characteristic scales of structural organization.

by an appropriate correlation length. The procedure of the correlation length estimation at $1/e$ level is shown in the same graph for one of the curves. Most of the ACF curves are characterized also by a subsequent series of maxima (sometimes not very well pronounced) with decaying amplitude, suggesting at least two levels of structural organization of structural subunits (systems with a hierarchy of structural organization). For ex-

ample, in the ACF curves for quasi-periodical arrangements of PS latex particles,¹² two levels of structural organization originated from two characteristic sizes present in the system: the latex particle diameter, and the average size of domains of a paracrystalline order. Most of the ACF curves calculated for our amorphous systems have similar features. As exemplified in Figure 5 for an ACF curve of PS 9M, the autocorrelation functions can be characterized by two length scales instead of simply a single correlation length. The first is defined from the initial (steep) decay of the ACF as a $1/e$ level, while the second one may be found from the position of the first-order maximum at the ACF curve.

The simulated structures show roughness at the level of the individual chains and on a larger scale, as can be seen by direct inspection of the models (Figure 6a). We can readily identify the chains ends and loops protruding from the surface. The effect of the surface on the chain orientation function can be seen in Figure 6b. The divergence of the lateral and perpendicular components close to the surface means that the chain envelope is effectively flattened close to the surface, in agreement with previous evidence about chains at interfaces.

The same two-level structural organization observed experimentally can be found for simulated surfaces. One of the ACF curves for simulated surfaces is shown together with corresponding ACFs extracted from the experiment in Figure 5b. Typically the larger-scale correlation is masked by the smaller one in this case

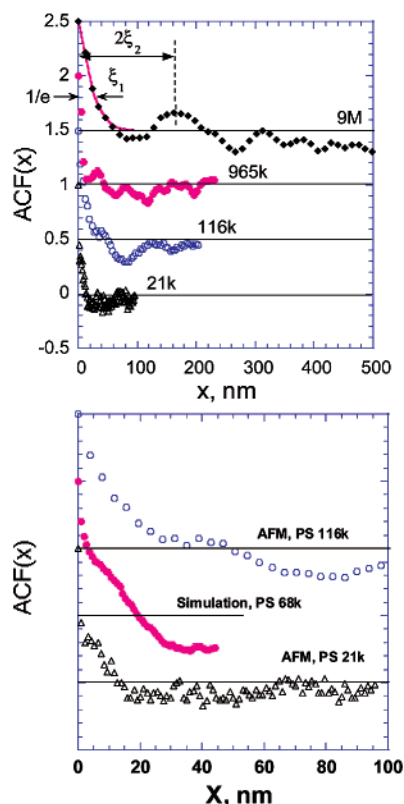


Figure 5. Autocorrelation functions calculated from the AFM images for different molecular weight PS samples (a). (The curves are shifted vertically for clarity.) Principle of the correlation length estimation as $1/e$ level of the exponential decay corresponding to the initial (steep) part of the ACF curve (solid line) and to the first-order maximum of characteristic oscillations is shown. These two approximations give two different levels of quantitative description of the system: the correlation lengths ξ_1 and long-range correlation parameter ξ_2 . Part b shows the initial parts for some of the experimentally determined ACF curves in comparison to the ACF calculated for simulated PS surface ($M_n = 68K$).

because of the limited number of segments being considered (relatively small “scan-size”). However, appropriate filtering of the image (smoothing by convolution either with a sphere imitating the tip shape, or with a simple rectangular function) allows visualization of this secondary structural correlation. An example of such a procedure is demonstrated in Figure 7. Here the initial autocorrelation function is plotted together with smeared functions, with a rectangular function of width 3, 5, or 7 data points. Part b of this figure demonstrates the fact that the original ACF and the smeared functions can be described as an exponential decay, at least for the initial slope ($x < 10$ nm). Therefore, a characteristic length scale of correlation can be defined in the same way as for experimental data as $1/e$ decay of the ACF(x). Also, we can see that the smearing procedure is not very sensitive to the width of the rectangular function used for convolution. Therefore, two characteristic length scales can be extracted from simulation results: ξ_1 for the initial unsmeared ACF, and ξ_2 for the smeared ACF (which may also imitate SFM image data). Despite the fact that simulation results cover only relatively short-chain systems, which were mostly inaccessible for SFM studies because of the lack of resolution (the SFM images are described as a convolution of the real surface with the probe tip shape, therefore masking fine details of the polymer structure), the comparison of Figures 5 and 7 gives a flavor of the

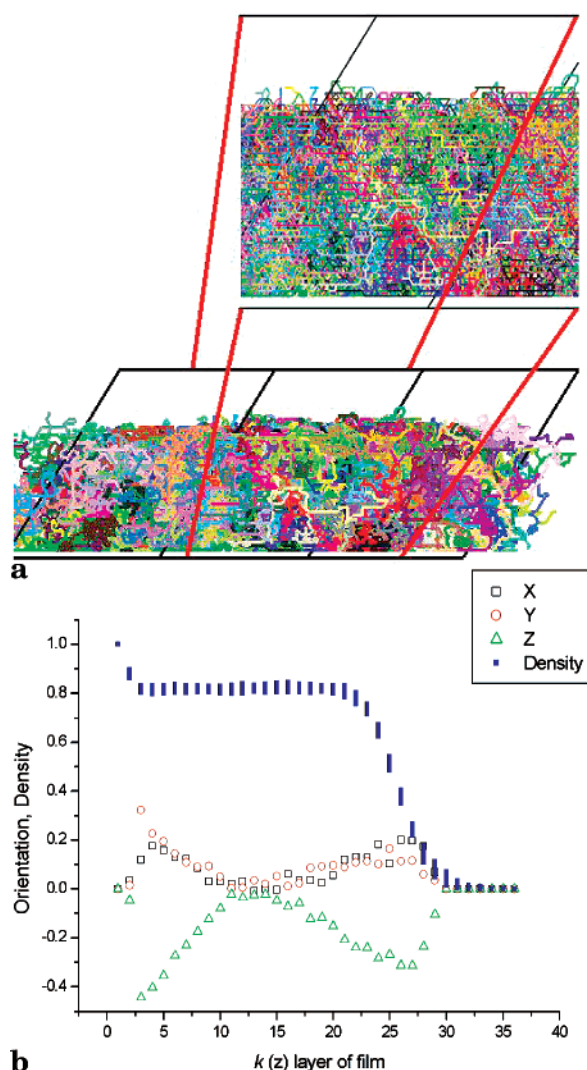


Figure 6. (a) Side view of a simulated surface, with a zoom-in to show chain detail. Note the roughness, and the chain ends protruding from the bulk. (b) Components of the orientation distribution (eq 5) along the surface (x, y) and perpendicular to the surface (z), throughout the simulated aPS film. Note the “flattening” of the chain envelope close to the surface. Inlaid with this is a density distribution of the chain throughout the simulated film.

similarity of all these systems, as well as of experimental and simulation results.

We summarize all the experimental and computer simulation results in Figure 8. Here we plot together the experimental correlation lengths (measured from the initial slope of the ACF or from the position of the first maximum) and the correlation length for simulated surfaces (the shortest one, measured directly from the ACF analysis, and the longer one being accessed only after cutoff of the shortest component by smoothing). The curve of calculated radii of gyration represents a natural length scale of the system. The graph can be divided into three main regions: a region of relatively small molecular weights (below $M_n \sim 70K$), a region of high molecular weights ($>200K$), and an intermediate region. Such a division relates to limitations of the methods applied. The first region is inaccessible for the SFM method due to tip–surface convolution, but is the most convenient range for computer simulations. The second region is very informative in experimental studies but is beyond the speed of modern computation

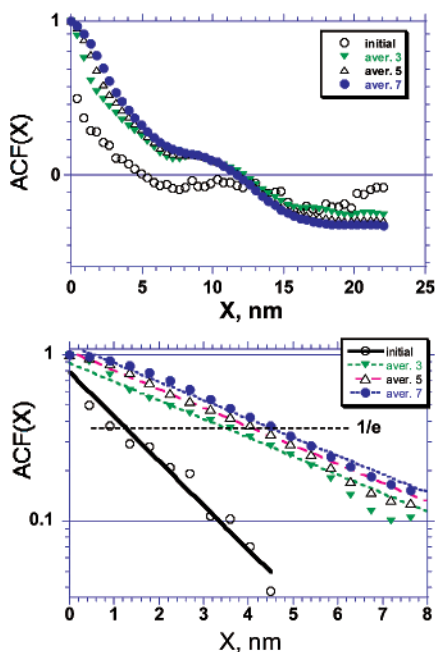


Figure 7. Principle of estimation of the same two correlation lengths as defined in Figure 5 from the simulated surface ACFs. Convolution with different size step functions allows a cutoff of the shorter correlation length typical for the original surfaces and efficient “unmasking” of the longer-range correlations. Both linear coordinate (a) and logarithmic scale (giving evidence of the exponential decay) representation (b) are presented.

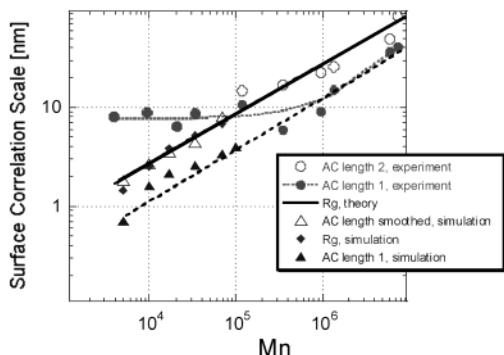


Figure 8. Summary graph of characteristic length scale parameters vs molecular weight found for amorphous polymer surface. Circles are for experimental (AFM) data: open circles—original AC length values (ξ_1), solid circles are ξ_2 , as illustrated in Figure 5. Open squares and solid triangles are correlation length calculated for raw simulated surfaces in two different simulation experiments, and open triangles the same for “smoothed” simulated surfaces (see description in the text). Diamonds represent theoretically calculated values of radius of gyration of polymer chains in an ideal random coil approximation. Solid lines correspond to the best linear fits of calculated values of ξ_2 and of the radii of gyration, and the dashed line corresponds to an interpolation fit of the ξ_1 found from experimental data and simulations. The dotted line is a guide for the eye line to describe ξ_1 values found from experimental data only.

possibilities. The intermediate region allows comparison of experimental and theoretical results.

The comparison of experimental ξ with simulated results suggests that the simulated polymer surfaces have at least 5 times higher “resolution” of polymer surface structure representation in comparison to real resolution achieved in our SFM experiments. Development of the mathematical procedure of deconvolution of the SFM tip shape with the surface relief is needed

for better comparison with the simulation results. On the other hand, further refinement of the simulation model and its “extension” to higher molecular mass polymer chains allowing more points of comparison with experiment and theoretical scaling laws is also desirable. For the PS fractions used in this study one can calculate R_g (radii of gyration) in a random coil approximation with a monomer size $a = 0.254$ nm and free volume parameter $C_\infty = 9.8$ as reported in the literature.¹⁶ The calculated values of R_g are plotted in Figure 8. One can notice a rather good agreement with the larger correlation length of height distribution found in both SFM experiments and independently from computer simulations.

Conclusions

We have studied free equilibrium state surfaces of polystyrenes with M_n in the range 3.9 kg/mol to 9 Mg/mol using scanning force microscopy. Height images were quantitatively characterized by means of an autocorrelation function analysis. We found an initial exponential decay followed by a series of peaks in the autocorrelation functions. Both the correlation length related to the initial decay, and the length scale given by the first peak position are found to scale in accordance with the size of polymer chains. The correlation length corresponds roughly to a submacromolecular scale (several monomer distances). The characteristic scale related to the first peak does in fact coincide numerically with the theoretical values of the radius of gyration. This is an entirely new finding, which however agrees well with earlier observations made by some of us on amorphous PMMA surface and PS latex nanoparticulate systems.¹² In the latter case the peak position was found to relate to the decay in the packing arrangement of latex particles into correlated domains.

The limitations of the methods are that the simulations can only reach up to molecular weight of 10^5 , due to the long relaxation times required, while the scanning force method is somewhat limited at molecular weights below 10^5 due to the convolution with the SPM tip size. However, since an overlap has been achieved, the simulation turns out to be a valuable extension of the experimental range and helps greatly in the interpretation of our findings.

We conclude that this study has given new insights into surface topography of amorphous polymer systems, validated coarse grained simulation techniques for probing polymer surface features on the nanometer scale, and therefore provides a new opening for further research in this important field. Future work will aim to extend the range of simulations in molecular weight, and will have to revisit the question of the scaling exponent on the surface, whether it is the same or different to that in the bulk.

Acknowledgment. Part of this work was carried out in the Oxford Toppan Centre, supported by the Toppan Printing Company. We thank the Cambridge HPCF for providing access to their computing facilities for this project.

References and Notes

- (1) *Physics of Polymer Surfaces and Interfaces*; Sanchez, I. C., Ed.; Butterworth-Heinemann: Boston, MA, 1992.
- (2) De Gennes, P. G. *Scaling Concepts in Polymer Physics*; Cornell University Press: Ithaca, NY, 1979.

- (3) Russ, J. C. *Fractal Surfaces*; Plenum Press: New York, 1994.
- (4) Meakin, P. *Fractals, scaling and growth far from equilibrium*; Cambridge University Press: Cambridge, U.K., 1998.
- (5) Strobl, G. *The Physics of Polymers*, 2nd ed.; Springer: Berlin, 1997.
- (6) Grosberg, A. Yu.; Khokhlov, A. R. *Giant Molecules. Here, there and everywhere...*; Academic Press: San Diego, CA, and London, 1997.
- (7) Sun, S. F. *Physical Chemistry of Macromolecules. Basic Principles and Issues*; John Wiley & Sons Inc.: New York, 1994.
- (8) Elias, H.-G. *An Introduction to Polymer Science*; Weinheim: New York, 1997.
- (9) Kirste, R.; Kruse, W. A.; Ibel, K. *Polymer* **1975**, *16*, 120.
- (10) *Scanning Probe Microscopy of Polymers*, Ratner, B. D., Tsukruk, V. V., Eds.; ACS Symposium Series 694; American Chemical Society: Washington, DC, 1998.
- (11) Haire, K. R.; Carver, T. J.; Windle, A. H. *Comput. Theor. Polym. Sci.* **2001**, *11* (1), 17.
- (12) Müller, M.; Wittmer, J. P.; Barrat, J.-L. *Europhysics Lett.* **2000**, *52*, 406.
- (13) Frank, C. W.; Rao, V.; Despotopoulou, M. M.; Pease, R. F. W.; Hinsberg, W. D.; Miller, R. D.; Rabolt, J. F. *Science* **1996**, *273*, 912.
- (14) Bliznyuk, V. N.; Burlakov, V. M.; Assender, H. E.; Briggs, G. A. D.; Tsukahara, Yu. Surface Structure of Amorphous PMMA from SPM: Auto-Correlation Function and Fractal Analysis, *Macromol. Symp.* **2001**, *167*, 89.
- (15) Guinier, A. *X-ray Diffraction in Crystals, Imperfect Crystals, and Amorphous Bodies*, W. H. Freeman, and Co.: San Francisco, CA, and London, 1963.
- (16) Sterrazza, M.; Xiao, C.; Jones, R. A. L.; Bucknall, D. G.; Webster, J.; Penfold, J. *Phys. Rev. Lett.* **1997**, *78*, 3693.
- (17) Bliznyuk, V. N.; Campbell, A.; Tsukruk, V. V. In *Organic Thin Films: Structure and Applications*; Frank, C. W., Ed.; ACS Symposium Series 695; Oxford University Press: Oxford, U.K., 1998; p 220.
- (18) *Polymers in Solutions: Theoretical Considerations and Newer Methods of Characterization*, Ed.; Forsman, W. C., Plenum Press: New York and London, 1986.

MA0119777